

REFERENCE

NBS
PUBLICATIONS

NAT'L INST. OF STAND & TECH



A11106 261094

HEAT CAPACITY MEASUREMENTS ON STRUCTURE I AND II
PURE HYDRATES AT LOW PRESSURES AND BELOW ROOM TEMPERATURE

FINAL REPORT
(October 1981-September 1982)

Gas Research Institute
8600 West Bryn Mawr Avenue
Chicago, Illinois 60631

QC
100
.U56
83-1682
1983



NBSR
05100
456
10.33-1652
1712

Heat Capacity Measurements on Structures I and II
Pure Hydrates at Low Pressures and Below Room Temperature

Final Report
October 1981 - September 1982

prepared by
J. E. Callanan and E. D. Sloan

Thermophysical Properties Division
National Bureau of Standards
Boulder, Colorado 80303

for

The Gas Research Institute

Contract Number 5081-360-0487

GRI Project Manager
Dr. Ferol Fish
Manager, Physical Sciences
Basic Research Department

LEGAL NOTICE

This report was prepared by J. E. Callanan and E. D. Sloan as an account of work sponsored by the Gas Research Institute ("GRI"). Neither GRI, members of GRI, nor any person acting on behalf of either:

- a. Makes any warranty or representation, express or implied, with respect to the accuracy, completeness, or usefulness of the information contained in this report, or that the use of any information, apparatus, method, or process disclosed in this report may not infringe privately-owned rights; or
- b. Assumes any liability with respect to the use of, or for damage resulting from the use of, any information, apparatus, method or process disclosed in this report.

REPORT DOCUMENTATION PAGE	1. REPORT NO. GRI-81/0102	2.	3. Recipient's Accession No.
4. Title and Subtitle Heat Capacity Measurements on Structure I and II Pure Hydrates at Low Pressures and Below Room Temperature		5. Report Date September 1982	
7. Author(s) J.E.Callanan and E.D.Sloan		8. Performing Organization Rept. No. NBSIR 83-1682	
9. Performing Organization Name and Address Thermophysical Properties Division National Bureau of Standards 325 Broadway Boulder, CO 80303		10. Project/Task/Work Unit No. 7730573	
		11. Contract(C) or Grant(G) No. (C) 5081-360-0487 (G)	
12. Sponsoring Organization Name and Address Gas Research Institute 8600 West Bryn Mawr Avenue Chicago, IL 60631		13. Type of Report & Period Covered Final October 1981 - September 1982	
15. Supplementary Notes		14.	
16. Abstract (Limit: 200 words)			
<p>World resources of natural gas in hydrate form are on the order of trillions of cubic meters. Thermophysical property measurements are vital to the determination of the exploitability of this resource. The natural gas hydrates are clathrates; the hydrate lattice exists in one of two special structures (I and II), both of which are different from any of the known forms of ice. The hydrate lattice forms with cavities or cages in which molecules in specific size ranges can be trapped. Heat capacities as a function of temperature and, where appropriate, heats of dissociation have been measured for tetrahydrofuran (II), ethylene oxide (I), and cyclopropane (I and II) hydrates by differential scanning calorimetry. The heat capacities were found to vary both with structure and with guest. Scanning calorimetric techniques and sample handling techniques suitable for dealing with hydrates in the subambient region were developed.</p>			
17. Document Analysis a. Descriptors			
Clathrate hydrates; cyclopropane hydrate; differential scanning calorimetry; ethylene oxide hydrate; heat capacity; heat of dissociation; tetrahydrofuran hydrate.			
b. Identifiers/Open-Ended Terms			
c. COSATI Field/Group			
18. Availability Statement: Release unlimited		19. Security Class (This Report)	21. No. of Pages
		20. Security Class (This Page)	22. Price

RESEARCH SUMMARY

Title Heat Capacity Measurements on Structure I and II Pure Hydrates at Low Pressures and Below Room Temperature

Contractor National Bureau of Standards
GRI Contract Number 5081-360-0487

Principal Investigators J. E. Callanan and E. D. Sloan

Report Period October 1981 - September 1982
Final Report

Objective To determine the heat capacity of structure I and structure II clathrate hydrates, to examine the effects of structure and guest on heat capacity, and to evaluate the utility of differential scanning calorimetry (DSC) for hydrate studies.

Technical Perspective Estimated world reserves of natural gas in hydrate form are on the order of 28 Tcm (1000 tcf) or more. The thermo-physical properties of these hydrates will be a key to resource determination and recovery. Recent measurements on some gas hydrates have shown the thermal conductivity to be anomalously low. As anomalies in the thermal conductivity often manifest themselves in the heat capacity, the measurement of hydrate heat capacities could provide guidance in the application of heat transport theory to hydrates. This information will help explain the reported thermal conductivity values and the understanding of heat transfer in dissociating hydrates into natural gas.

In the gas hydrates, the hydrate lattice generally forms in one of two structures, both of which are different from ordinary ice. These structures differ principally in the number of water molecules per unit cell and in the number and size of the cavities formed. The substances enclosed in the cavities at the time of formation are commonly referred to as guests.

Results Heat capacities and heats of dissociation were measured in sealed specimen cells by differential scanning calorimetry for hydrates of tetrahydrofuran (THF), ethylene oxide (EtO), and cyclopropane (Cy); two guests each were studied in both structures I and II. The guest appears to have a significant effect (5 - 9 percent) on heat capacities of both structures. For the same guest, cyclopropane, the heat capacities are significantly different for the two different structures.

Appropriate methods for the use of differential scanning calorimetry for hydrate studies have been developed.

Technical Approach As natural gas hydrates, which are of primary interest, are difficult to prepare satisfactorily in the laboratory, the study of the heat capacity of these substances was approached through the study of tetrahydrofuran, ethylene oxide, and cyclopropane hydrates. Ethylene oxide forms a structure I hydrate, tetrahydrofuran, structure II; cyclopropane hydrates can form in either structure I or II, depending on formation conditions. Natural gas hydrates occur most frequently as structure I hydrates; however, in permafrost regions the natural gas hydrates will form in structure II if propane is present.

The methods of hydrate and specimen preparation varied for each hydrate. The heat capacities and heats of dissociation were measured in a differential scanning calorimeter (DSC) in the general temperature range 240-300 K. The temperature calibration of the instrument was set with indium and water; sapphire and indium/water were used as heat capacity and transition standards.

The accuracy of the DSC for use in the scanning mode to determine heat capacity was established as better than two percent by comparison of measured heat capacities of potassium chloride with results obtained by classical calorimetry. All weighings were done on a microbalance accurate to five micrograms as determined by comparison with weights calibrated by the National Bureau of Standards (NBS). The data were corrected for calibration information; a generalized correction for specimen pan mass was applied.

**Project
Implications**

The light compounds in natural gas combine with water at elevated pressures and low temperatures to form a solid compound known as a clathrate hydrate. Since hydrates were first determined to occur in gas transmission lines, some fifty years ago, hydrate thermodynamic studies were undertaken to find ways to mitigate their formation. It is now recognized that the natural occurrence and formation of gas hydrates need to be taken into account in exploration, drilling, and production in regions of permafrost or deep oceans. A growing amount of information suggests that hydrates are common in nature and constitute a potential supply of substantial quantities of gas. Significant gaps exist in our basic knowledge of hydrates. These gaps include their thermal properties, on which this contract was focused.

Only a limited number of hydrates were examined in this study, but the techniques employed and results obtained should be applicable to other systems that also deserve study. Cyclopropane was chosen as a guest molecule because

it is rare in forming both hydrate structures. In addition, like ethylene oxide and tetrahydrofuran, it forms hydrate at low pressures so that high-pressure apparatus was not required for this study. A substantial portion of the investigation was spent in developing experimental techniques for heat capacity and heat of dissociation measurement by DSC, particularly at subambient conditions. The heat capacity differences shown in these initial results warrant confirmation with other hydrates, perhaps with guests of different sizes.

GRI Project Manager
Ferol Fish
Manager, Physical Sciences

TABLE OF CONTENTS

INTRODUCTION	1
OVERALL PROJECT OBJECTIVE	1
BRIEF DESCRIPTION OF THE PROJECT	1
RATIONALE FOR UNDERTAKING THE PROJECT	1
PROJECTED BENEFITS TO GAS CONSUMERS	2
TECHNICAL SECTION	2
WORK PLAN	2
WORK PERFORMED	2
CALORIMETRY	2
Instrumentation	2
Specimen Selection	2
Procedures	3
Data Reduction	4
ETHYLENE OXIDE HYDRATES	4
Background Information	4
Sample and Specimen Preparation	4
Measurements	5
Results and Discussion	5
TETRAHYDROFURAN HYDRATES	6
Background Information	6
Sample and Specimen Preparation	6
Measurements	6
Results and Discussion	7

CYCLOPROPANE HYDRATES	8
Background Information	8
Sample and Specimen Preparation	8
Measurements	9
Results and Discussion	9
MAJOR ACHIEVEMENTS OF THE PROJECT	9
MAJOR TECHNICAL PROBLEM AREAS ENCOUNTERED	10
RECOMMENDATIONS	10
REFERENCES	11
LIST OF TABLES	12
LIST OF FIGURES	17

INTRODUCTION

Clathrate hydrates are inclusion compounds in which the host is an ice lattice and the encaged guest is a gas or a liquid. The host lattice in the hydrate belongs to either structure I or structure II as determined by von Stackelberg (6). Both of these lattice structures contain cavities of different sizes which can accommodate guests of different sizes. The small cages are nearly the same size in each; the large cage radii differ only slightly but this difference has a significant effect on the guest accommodated.

The natural gas hydrates are clathrate hydrates. They were viewed as a laboratory curiosity or a processing/transport nuisance until it was determined recently that significant amounts of natural gas may exist in hydrated form over large areas of the earth's permafrost regions and under the ocean floor. Thermal property data will be required for the evaluation of methods of exploitation of this resource.

OVERALL PROJECT OBJECTIVE

The object of this investigation was to determine the heat capacities of structure I and structure II clathrate hydrates, to examine the effects of structure and guest on heat capacity, and to evaluate the utility of differential scanning calorimetry (DSC) for hydrate studies.

BRIEF DESCRIPTION OF THE PROJECT

Because homogeneous hydrates form readily when the guests are completely miscible with liquid water, ethers were used as hydrate formers: ethylene oxide (EtO) for structure I and tetrahydrofuran (THF) for structure II. After obtaining heat capacity and dissociation data for each structure using different guest molecules, heat capacities were obtained for cyclopropane, a guest molecule which occupies either of the two structures, depending on its formation temperature (7). In this manner, an attempt was made to determine the effect of hydrate structure on heat capacity, independent of guest molecule. In addition, procedures for scanning calorimetry, suitable for use in hydrate studies, have been developed.

RATIONALE FOR UNDERTAKING THE PROJECT

Thermal property data will be required no matter whether thermal stimulation, pressure reduction, or antifreeze injection is deemed to be the most suitable technique for the recovery of gas from hydrate zones. The hydrates used in this study are more readily prepared than the natural gas hydrates, but do provide the needed information about the effects of structure and of guest on heat capacity and/or heat of dissociation.

The composition of both the natural hydrate and its matrix (sediment, minerals) will vary because of the manner and site of its formation. Therefore, as with similar naturally occurring materials, replicate samples should be used to account for possible heterogeneity. The techniques of differential scanning calorimetry are ideally suited to repeated, relatively rapid measurements of multiple specimens. The small specimen size, usually less than 10 milligrams,

will be especially suitable for work with natural hydrates, as such samples are both difficult and expensive to obtain.

PROJECTED BENEFITS TO GAS CONSUMERS

As estimated world reserves of natural gas in hydrate form are on the order of 28 Tcm (1000 tcf) or more, the thermophysical properties of these hydrates will be a key to resource determination and recovery.

TECHNICAL SECTION

WORK PLAN

All hydrate samples were prepared at Colorado School of Mines; details of the preparation will be found in the technical sections dealing with the individual hydrates. The use of a DSC for determining the heat capacity of hydrates was evaluated and suitable procedures for dealing with hydrates were developed. Heat capacities and, where appropriate, heats of dissociation were measured in sealed cells by DSC, at the National Bureau of Standards (NBS).

WORK PERFORMED

CALORIMETRY

Instrumentation

The scanning calorimeter used in this study was a Perkin-Elmer, DSC-2C with associated automation devices, also supplied by Perkin-Elmer;¹ this equipment is located at the National Bureau of Standards in Boulder, Colorado.

Commercial scanning calorimeters in use today require standards to establish absolute values for the quantities measured. In this work, Calorimetry Conference sapphire was used as a heat capacity standard; indium was used as the primary transition standard. Deionized distilled water was used as an auxiliary standard for both measurements.

The accuracy of this instrument for use in the scanning mode to determine heat capacity was established as better than two percent by comparison of measured heat capacities for potassium chloride with results obtained by classical calorimetry by Berg and Morrison (3), and by Douglas and Harmon (4). All weighings were done on a microbalance accurate to five micrograms as determined by comparison with weights calibrated by the NBS.

Specimen Selection

Through work with the THF hydrate, chronologically the first hydrate studied, it was noted that the dissociation curves could be used to identify the regions of the phase diagram to which a particular hydrate specimen belonged. That is, samples in the THF study corresponded to three regions of the

¹The use of trade names does not constitute an endorsement of any manufacturer's equipment. Their use is necessary to properly evaluate and apply the results of this study.

phase diagram given by Dyadin (5) for THF-water at one atmosphere, which is shown in Figure 1: (a) 2, the line representing hydrate only; b) region 4, in which premelting would be expected; and c) region 5, where a eutectic halt as well as hydrate dissociation will be observed. A specimen with only hydrate would decompose (or melt) sharply as would any pure substance. A typical scan is shown in Figure 2. A specimen from region 5 would contain a eutectic mixture of hydrate and ice; a typical dissociation curve for this system, given in Figure 3, would show two peaks, one for eutectic melting and one for dissociation. Figure 4 illustrates the dissociation curve from region 4, where a premelting-like phenomenon is observed.

Specimens for all three regions were studied, but only that corresponding to the composition of the hydrate line is considered "pure" hydrate.

Procedures

The specimens were placed in sealed aluminum capsules which had been treated to make the aluminum resistant to reaction with water. The sealed capsules were sometimes kept at sub-zero temperatures until placed in the calorimeter, and at other times were allowed to warm to room temperature, and subsequently cooled at 320 K per minute. Because of the well-known problems with metastability encountered in the measurements of the heat capacity of ice (6), the hydrates formed as a result of cooling at 320 K per minute, 5 K per minute, and 0.31 K per minute were compared. The variations in the heat capacity of the 4.47 mg specimen studied in this manner were within the limits of precision of the DSC as noted above.

In the normal measurement sequence, the baseline and the calibration of the instrument were checked. An empty sample pan and the sapphire standard were run over the required temperature range. Water was run in the heat capacity mode up to 270 K; the specimen was then cooled to 260 K, and a fusion or dissociation run made. This procedure was required by the electronics of the data acquisition system. A scan begun close to a transition was subject to electronic effects which could alter the transition temperature. Each hydrate specimen was run in the same manner with the high end of the heat capacity scan being governed by the dissociation conditions for that particular hydrate.

In a few instances, a heat capacity scan which appeared to proceed satisfactorily, gave values for the heat capacity which differed from those of other, presumably similar, specimens by as much as ten percent. Invariably an examination of the dissociation scans for these specimens revealed anomalies; the specimens in question were considered to be unsatisfactory and data for them are not presented here.

It was noted that runs repeated on the same specimens of EtO hydrate over a period of months gave results for heat capacities which became progressively lower even though the sample mass had remained unchanged. One possible explanation of these marked progressive changes lay in the interaction of the hydrates with the pan material. Though the aluminum cells had been treated to make them resistant to attack by water, apparently this resistance breaks down after a period of months. Though the samples were stored over this period of time as solid hydrates, no other explanation of the change in heat capacity of a closed system without an accompanying change in mass was obvious. Accordingly, three specimens were opened and the pans examined under a microscope.

In all cases the pans showed evidence of attack by the specimens; this attack was most serious in the case of a specimen of water which had been kept at room temperature for several months. Photomicrographs of the pans are shown in Figure 5.

In summary of the effects described here, specimens with anomalous dissociation curves inevitably had anomalous heat capacities. However, some specimens for which dissociation temperatures and energies were acceptable, showed significant progressive changes in heat capacity; in these instances the specimen pan material had deteriorated. Thus it appears that acceptable dissociation curves are necessary, but not sufficient, for acceptable heat capacities. Heat capacities are seen to be much more sensitive to sample/specimen variation than fusion temperatures and energies, as evidenced above.

Duplicate runs on the same sample agreed well; precision of the heat capacity measurements was 1.6 percent or better. Agreement between replicate samples depended on the specific hydrate and the manner of specimen preparation; this will be discussed in the appropriate sections of this report.

Data Reduction

A polynomial in temperature was fitted to the heat capacities for each hydrate; the optimum form for the analytical expression was selected from the statistical analysis. Dissociation energies were obtained through the automated data acquisition system; a previous study with indium had found the results to have a precision of 0.33 J g^{-1} .

ETHYLENE OXIDE HYDRATES

Background Information

The phase diagram for ethylene oxide and water at 101.32 kPa is shown in Figure 6. The vapor-liquid envelope exists just above the liquid-hydrate boundary. Ethylene oxide-water liquid mixtures are completely miscible between the two-phase regions.

The hydrate forms in structure I with the EtO guests occupying essentially all of the large cavities and some of the small ones. The ideal hydrate composition, as reported by Glew (7), is shown as the vertical line at a composition of approximately 0.125 mole fraction. The maximum temperature at the ideal hydrate composition is 284.2 K. The various areas of this phase diagram are labeled according to the usual convention. For readers not familiar with this convention, a two-phase mixture of hydrate and liquid exists to the right of the hydrate line. To the left of the hydrate line and below the eutectic, a solid mixture of hydrate and ice exists. To the left of the hydrate line and above the eutectic are two, two-phase regions; ice and liquid on the left (A) and a larger region of hydrate and liquid (B) on the right.

Sample and Specimen Preparation

The sample preparation apparatus was essentially that described by Dharmawardhana (8) with the important exception that all of the copper inlet

lines were exchanged for stainless steel, for safety considerations. The apparatus consists of a temperature-controlled, ultrasonically-agitated bearing bronze cell which is connected to the makeup chemical container through a piston displacement chamber.

Samples were prepared from doubly-distilled water and 99.9 percent pure research grade ethylene oxide. The ethylene oxide was condensed into the cell and then placed in a stoppered bottle before adding the water. Samples close to the ideal composition were prepared by volume; the compositions were verified by mass measurements accurate to 0.01 percent. The frozen samples were transported to the NBS before encapsulation.

Individual specimens were prepared by cutting pieces of about 6 mg each from the bulk solid sample; these were sealed in air in aluminum specimen containers before further refrigeration.

Measurements

The optimum ethylene oxide hydrate sample was determined from its dissociation curve. Two specimens close to the optimum composition, but with a negligible amount of premelting, were measured for heat capacity and heat of dissociation over a five-month period. The temperature range of the heat capacity scans was 240-270 K. One of these samples, E2, was run in duplicate to verify instrument precision. Two other specimens, from the eutectic side of the ideal hydrate composition, were also studied.

Results and Discussion

Specimens E2 and E5 were from the sample close to the optimum composition; E21 and E22 were duplicate runs on specimen E2. The dissociation scans for these specimens had a single peak. Specimens E3 and E4 were from the sample on the eutectic side of the ideal hydrate composition; as expected, they exhibited two peaks in their dissociation scans. The experimental data for the EtO hydrates are given in Table 1.

For the EtO one-peak scans, the average heat of dissociation was 295.0 J g^{-1} ; the difference between the largest and smallest values was 1.2 percent. The heat capacity curve generated by the data reduction program is shown in Figure 7; the deviation plot for this system is given in Figure 8. The statistical regression of the data yielded the equation

$$C_p = 4.0300 - 0.026117 T + 0.704050 \times 10^{-4} T^2 \quad (1)$$

with a root mean squared deviation of 0.115×10^{-1} . The heat capacity and root mean squared deviation (rmsd) for Equations 1-8 are given in millijoules/milligram K; T is in Kelvin. The largest variation in these data occurs at 255 K where the deviation between the largest and the smallest values is 1.5 percent. The agreement between duplicate runs is shown in Table 1. No heat capacity or heat of dissociation data were found in the literature for comparison.

For the sample with admixed ice, E3 and E4, the heats of dissociation have little meaning because of the presence of the eutectic peak. The heat capacities of these specimens, as shown in Table 1, are higher than those discussed

above and close to those of ice (6). The smoothed heat capacity curve for E3 and E4 is also indicated in Figure 7 so that a comparison may be made for the different hydrate samples. For the two-peak EtO specimens, the equation obtained was

$$C_p = 4.4602 - 0.028414 T + 0.73636 \times 10^{-4} T^2 \quad (2)$$

with a root mean squared deviation of 0.220×10^{-1} .

TETRAHYDROFURAN HYDRATES

Background Information

Tetrahydrofuran hydrate, a structure II hydrate, was first reported by Palmer (9), who determined the composition to be between 13 and 16 host molecules of water for each guest molecule of THF. Erva (10) considered the ideal hydrate composition to be 16:1. Gough and Davidson (11), who studied hydrate composition as a function of density, considered the ideal composition ratio to be closer to 17:1. It is this composition ratio which is considered to give hydrate only in this study. The phase diagram for the THF-water system at atmospheric pressure is shown in Figure 1. This phase diagram is labeled in the conventional way, as discussed under EtO hydrate. The THF guest occupies only the larger cages in structure II.

Sample and Specimen Preparation

The samples were prepared as liquid mixtures from doubly-distilled water and 99.98 percent pure tetrahydrofuran; the impurity was mainly antioxidant. Five samples within 0.02 mole fraction of the composition of 17:1 (water:THF) were prepared by volume. The compositions were determined by mass measurements accurate to 0.01 percent. Approximately 6 microliters of each sample was loaded by microsyringe into an aluminum pan and sealed.

The dissociation scans were used to determine the region of the phase diagram represented by each specimen. Of the specimens reported here, two had compositions on, or very close to, the hydrate composition line, T1 and T2. Three were from region 4 of the phase diagram and therefore exhibited some pre-melting; these are labeled T3, T4, and T5. Specimens T6 and T7 were from region 5 and show a eutectic effect.

Measurements

Since this system consisted of two miscible liquids above the dissociation region, no attempt was made to keep the specimens at subambient temperatures during the calorimetric measurements. The specimens were placed in the calorimeter at about 280 K and cooled at 320 K per minute to 240 K. No evidence of solidification was noted in the system until about 250 K. This was true even when the specimens were cooled at 0.31 K per minute. Since the eutectic and dissociation temperatures were over 270 K, this behavior represented marked supercooling of the hydrates. As with the EtO hydrates, the temperature range for the heat capacity scans was 240-270 K.

Results and Discussion

The experimental data for the THF hydrates are given in Tables 2 and 3. As the temperatures for some of this work differed significantly from the nominal temperatures, the actual temperature of those measurements is noted in the Table. The heat capacity of ice at the various temperatures used in this study, interpolated from the data of Giaque (6), are also given in Table 2 for reference.

For the THF one-peak scans, the average heat of dissociation was 265.6 J g^{-1} ; the difference between the largest and smallest values was 1.4 percent. The heat capacity scan generated from the experimental data is given in Figure 9; Figure 10 shows the percent deviations for these measurements. The equation representing these results is

$$C_p = 6.1926 - 0.044729 T + 0.10899 \times 10^{-3} T^2 \quad (3)$$

with a root mean squared deviation of 0.203×10^{-1} .

While Table 3 lists the individual values of the specimens which showed premelting, the curve representing these specimens was obtained from the averaged values. For purposes of comparison with the other hydrate samples, this curve is also shown in Figure 9. It should be noted that in preparing these specimens a portion of the sample was removed and deliberately allowed to remain open to the atmosphere for a few minutes while the specimens were being prepared. However, these three specimens had very similar dissociation curves. The variations noted in the heat capacity are believed to be due to small variations in composition. This is further evidence that heat capacity is far more sensitive to variations in composition than is temperature or energy of dissociation.

The equation representing the heat capacity for these specimens is

$$C_p = 13.834 - 0.10884 T + 0.24286 \times 10^{-3} T^2 \quad (4)$$

with a root mean squared deviation of 0.588×10^{-2} .

In Figure 11 are shown the smoothed heat capacity curves for THF specimens from region 5 on the phase diagram, those which should show a eutectic effect. The curve for hydrate only is included also. The results for the two-peak specimens bracket that for pure hydrate. Equations for these two specimens are:

$$T6 \quad C_p = 4.9555 - 0.033594 T + 0.85714 \times 10^{-4} T^2 \quad \text{rmsd } 0.426 \times 10^{-2} \quad (5)$$

$$T7 \quad C_p = 39.687 - 0.30766 T + 0.62286 \times 10^{-3} T^2 \quad \text{rmsd } 0.490 \times 10^{-2} \quad (6)$$

The reasons for this discrepancy remain unresolved; hypotheses explaining it which include effects of metastability or incomplete transformation will be investigated.

The eutectic temperature obtained in this study, $271.9 \pm 0.3 \text{ K}$, agrees well with that cited by Cook and Laubitz (12) for the 'thermal anomaly', 271.65 K . This number was obtained from dissociation scans of several samples

with varying composition within region 5 in addition to the data given in the Table. The average melting point for the hydrates, T1 and T2 is 277.6; specimens containing admixed ice, which are similar to that used by Cook and Laubitz, dissociated at 277.0 K. Cook and Laubitz cite a melting range of 2.2 K, from 275.2-277.7 K. The heat capacities obtained in this study for the specimens considered to be hydrate only are about 13-14 percent higher than those of Cook and Laubitz, which are given for 268-271 K. At 260 K the heat capacities are 10 percent higher than those established from the curves given by Ross and Andersson (13) for volumetric heat capacity. However, the specimens studied by both these investigators were from region 5 of the phase diagram. If we compare their values given for sample T7, which was comparable, our values for heat capacity are four percent higher than Ross and Andersson at 260 K and 12.9 higher than those of Cook and Laubitz at 270 K. T7 was used for comparison because the results, lower than for hydrate only, are in accord with an auxiliary study of the variation of heat capacity with composition in region 5.

CYCLOPROPANE HYDRATES

Background Information

The phase diagram for cyclopropane vapor-hydrate-liquid water three phase mixtures is presented in Figure 12. This diagram differs markedly from the phase diagrams given for THF-water and EtO-water systems in that the lines of Figure 12 indicate the pressures and temperatures at which three phases (hydrate, vapor, and liquid water) coexist at equilibrium. At conditions of lower temperature or higher pressure than the line indicated hydrates will be in equilibrium with the excess phase, either vapor or water. Cyclopropane forms an unusual hydrate, however, because it is one of the few to form either structure, I or II, as a function of temperature (2). The temperature and pressure regions of stability for each structure are indicated in the Figure.

Sample and Specimen Preparation

The apparatus used for sample preparation is that described for EtO hydrates. The cyclopropane used was research grade (99.99 percent), which had previously been determined to be chromatographically pure. Structure I hydrates were made at a temperature of 280 K and structure II at 268 K, each at the corresponding equilibrium pressure shown in Figure 12. The water in the equilibrium cell was overpressured with cyclopropane vapor so that hydrates formed under the presence of ultrasonic agitation. Mathematical models by Dharmawardhana (8) indicate that more than 90 percent of the available large cavities are filled in either structure under these conditions.

The samples were subcooled, chipped from the cell, and transported to NBS at the normal sublimation temperature of carbon dioxide. An effort was made to cut flat solid pieces of about 6 mg each from the bulk samples for placement in DSC specimen containers, which were then sealed. It was necessary to keep everything which came in contact with the specimens very cold in order to prevent specimen decomposition and/or deterioration. These cyclopropane specimens were kept at all times at temperatures well below their expected dissociation temperatures.

Measurements

Heat capacities for these specimens were measured from 230 K up to the temperature at which the heat capacity scan began to rise steeply, indicating dissociation. For the sake of uniformity, data are reported over the same temperature ranges used for the other hydrates. Heats of dissociation are not considered meaningful for these hydrates since they dissociate to two phases, vapor and water, rather than a single miscible liquid as for the THF and EtO hydrates. The dissociation curve is of some value, however, in that the temperature of onset of dissociation gives an indication of sample homogeneity.

Results and Discussion

The structure I heat capacities data, given in Table 4 and Figure 13, show good agreement. Three specimens were measured, C4, C5, and C6. Duplicate runs for C5 are labeled C51 and C52; these indicate an instrument precision of 1.1 percent. The largest variation among runs occurs at 260 K, 5.3 percent where the heat capacity is rising very rapidly, perhaps indicating incipient dissociation in specimen 6. The equation which represents these data is

$$C_p = 0.16606 \times 10^4 + 0.25727 \times 10^2 T - 0.14898 T^2 + 0.38233 \times 10^{-3} T^3 - 0.3667 \times 10^{-6} T^4 \quad (7)$$

with a root mean squared deviation of 0.546×10^{-1} . The heat capacity curve is given in Figure 13.

Data for the structure II heat capacity are also given in Table 4 and Figure 13. The greatest variation in these results is seen at 240 K, 6.4 percent. The equation which represents these data is

$$C_p = -1.7196 + 0.01518 T - 0.92732 T^2 \times 10^{-6} \quad (8)$$

with a root mean squared deviation of 0.290×10^{-1} . The heat capacity curve for the structure II hydrates is also shown in Figure 13.

It is evident from Figure 13 that the heat capacities for structure II Cy hydrates are 13-18 percent higher than those for structure I with the same guest molecule. This indicates that the water structure has a significant effect on the heat capacity when the hydrate guest molecule does not change. No data for the heat capacities of cyclopropane are available in the literature for comparison.

MAJOR ACHIEVEMENTS OF THE PROJECT

Heat capacities and heats of dissociation have been measured in sealed specimen cells by differential scanning calorimetry for hydrates of tetrahydrofuran (THF), ethylene oxide (EtO), and cyclopropane (Cy); thus two guests each have been studied in both structures I and II. The guest appears to have a significant effect (5 - 9 percent) on heat capacities of hydrates of both structures. For the same guest, cyclopropane, the heat capacities are also significantly different for the two different structures.

Appropriate methods for the use of differential scanning calorimetry for hydrate studies have been developed.

MAJOR TECHNICAL PROBLEM AREAS ENCOUNTERED

1. Problems associated with specimen preparation include difficulties associated with a) filling cells with a liquid sample containing volatile liquid with no consequent change in the sample composition; b) cutting appropriately shaped solid specimens at temperatures around 200 K.

2. Problems were encountered in weighing specimens, at ambient temperature and humidity, which had been stored at 80 K or 196 K; these low storage temperatures were used to preclude specimen deterioration between preparation and measurement.

3. For the preparation of the ethylene oxide samples, the sample preparation apparatus needed to be reconstructed to eliminate possible interactions with copper, which is cited as a hazard in the use of ethylene oxide. In addition, the ethylene oxide was found to attack both Plexiglass² and Lexan;² this necessitated a reconstruction of the apparatus sight glasses to minimize contact with ethylene oxide.

4. The application of the DSC in the subambient region presented numerous difficulties, many of which were overcome. These included problems with ice formation in the calorimeter or its associated gas lines; the unavailability of calibration standards in the subambient region; and the application of correction factors.

RECOMMENDATIONS

Other hydrate systems of both structures should be studied to verify the effect of the guest on the structure II heat capacities and the effect of structure on heat capacity of a hydrate with a single guest, as was found for cyclopropane hydrates. Further studies should include guests representing other types of compounds. Also, study of the C₃ ether might illuminate the differences noted in this study due to the guest. The connection between irregular fusion scans and heat capacity values which vary far beyond the precision of the instrument should be elucidated.

It would be advisable in further studies to extend the lower end of the temperature range. In order to study the transition from structure I to structure II with cyclopropane the sample must be prepared and loaded into the cells at higher pressures. This capability, as well as one for high pressure calorimetry, would increase the information available to us. As the naturally occurring gas hydrates presumably form over long periods of time, further studies of the stability of relatively quickly formed hydrates should be conducted.

²The use of trade names does not constitute an endorsement of any manufacturer's equipment. Their use is necessary to properly evaluate and apply the results of this study.

REFERENCES

1. von Stackelberg, M. and Muller, H. R., Z. Elektrochem., 1954, 58, 25.
2. Hafemann, D. R. and Miller, S. L., J. Phys. Chem., 1969, 73, 1392.
3. Berg, W. T. and Morrison, J. A., Proc. R. Soc. London Ser. A, 1957, 242, 467.
4. Douglas, T. B. and Harmon, A. W., J. Res. Nat. Bur. Stand. Sect. A, 1974, 78, 515.
5. Dyadin, Y. A., Kuznetsov, P. N., Yakolev, I. I., and Pyrinova, A. V., Dokl Akad. Nauk SSSR, 1973, 208, 103.
6. Giaque, W. F. and Stout, J. W., J. Am. Chem. Soc., 1936, 58, 1144.
7. Glew, D. N. and Rath, N. S., J. Chem. Phys., 1966, 44, 1710.
8. Dharmawardhana, P. B., Parrish, W. R., and Sloan, E. D., Ind. Eng. Chem. Fund., 1980, 19, 410.
9. Palmer, H. A., Ph.D. Thesis, 1950, University of Oklahoma.
10. Erva, J., Suom. Kemistil. B, 1956, 29, 183.
11. Gough, S. R. and Davidson, D. W., Can. J. Chem., 1971, 49, 2691.
12. Cook, J. G. and Laubitz, M. J., Proc. Seventeenth International Thermal Conductivity Conf., June 1981 (in press).
13. Ross, R. G. and Andersson, P., Can. J. Chem. 1982, 60, 881.
14. Coles, K. F. and Popper, F., Ind. Eng. Chem., 1950, 42, 1434.
15. Maass, D. and Boomer, E. H., J. Am. Chem. Soc., 1922, 44, 1709.

LIST OF TABLES

Table 1. Experimental data for ethylene oxide hydrates.

Table 2. Experimental data for tetrahydrofuran hydrates: hydrate only; eutectic mixtures.

Table 3. Experimental data for tetrahydrofuran hydrates with premelting.

Table 4. Experimental data for cyclopropane hydrates.

Table 1

Experimental data for ethylene oxide hydrates.

Temperature, K	Heat Capacities, $J g^{-1} K^{-1}$					Percent Deviation E_{11}, E_{12}	Two Peaks	
	E_{21}	One Peak E_{22}	E_5	E_3	E_4			
245	1.86	1.85	1.86	1.92	1.93	0.64		
250	1.93	1.91	1.89	1.94	1.96	0.52		
255	1.97	1.94	1.94	1.98	1.99	1.5		
260	2.01	1.99	2.01	2.08	2.05	1.1		
265		2.06	2.05	2.15	2.07			
270				(2.32)	2.14			
T, K	284.7	284.6	283.1	281.9	N.A.			
$\Delta H, J g^{-1}$	294.1*	293.7*	297.3	(eutectic) 269.7	N.A.			

*Energy correction estimated.

Table 2

Experimental data for tetrahydrofuran hydrates: hydrate only; eutectic mixtures.

Temperature, K	Heat Capacities, $J g^{-1} K^{-1}$					
	One Peak			Two Peaks		
	T ₁	T ₂	Ice (9)	T ₆	T ₇	
245	1.77		1.90	1.87		
248.5		1.80	1.92		1.69	
250	1.85		1.93	1.91		
253.5		1.84	1.96		1.73	
255	1.91		1.97	1.97		
258.5		1.89	2.00		1.77	
260	1.94		2.01	2.01		
263.5		1.95	2.03		1.86	
265	1.99		2.04	2.08		
268.5		2.06	2.07		1.99	
			Dissociation			
T, K	278.1	277.1	273.15	(281.9)	(277.7)	
ΔH , $J g^{-1}$	267.3	263.8	333.7	N.A.	N.A.	
T, K (eutectic)				277.7	277.4	

Table 3

Experimental data for tetrahydrofuran hydrates with premelting.

T, K	Heat Capacities, $J g^{-1} K^{-1}$					Deviation
	T3	T4	T5	Percent		
245	1.76	1.68	1.79		3.3	
250	1.82	1.76	1.85		2.5	
255	1.87	1.82	1.90		2.2	
260	1.97	1.91	2.00		2.3	
265	2.05	1.98	2.11		3.2	
270		(2.30)	(2.47)			
T, K	277.3	Dissociation		276.1	0.2	
		276.2		248.3	1.9	
$\Delta H, J g^{-1}$	257.4	249.8				

Table 4

Experimental data for cyclopropane hydrates.

T, K	Heat Capacities, $J g^{-1} K^{-1}$						
	Structure I			Structure II			
	C4	C51	C52	C6	C1	C2	C3
240	1.62	--	--		1.82	1.94	1.87
245	1.67	1.63	1.64	1.72	1.92	1.96	1.93
250	1.75	1.66	1.67	1.75	1.99	2.02	2.02
255	1.84	1.71	1.70	1.82	2.06	2.10	2.10
260	--	1.78	1.80	1.96	2.16	2.19	2.20
265	--	--	--		2.22	--	--

LIST OF FIGURES

- Figure 1. Phase diagram for tetrahydrofuran-water system at one atmosphere.
- Figure 2. DSC scan typical of pure substance (hydrate only).
- Figure 3. DSC scan of specimen from eutectic region.
- Figure 4. DSC scan of specimen showing premelting.
- Figure 5. Photomicrographs of specimen pans illustrating deterioration (50X).
- Figure 6. Phase diagram for ethylene oxide-water system (14, 15).
- Figure 7. Heat capacity versus temperature-ethylene oxide hydrates.
- Figure 8. Deviation plot for ethylene oxide hydrates.
- Figure 9. Heat capacity versus temperature-tetrahydrofuran hydrates.
- Figure 10. Deviation plot for tetrahydrofuran hydrates.
- Figure 11. Heat capacity versus temperature-tetrahydrofuran eutectic mixtures.
- Figure 12. Dissociation pressure curve for cyclopropane hydrate.
- Figure 13. Heat capacity versus temperature-cyclopropane hydrates.

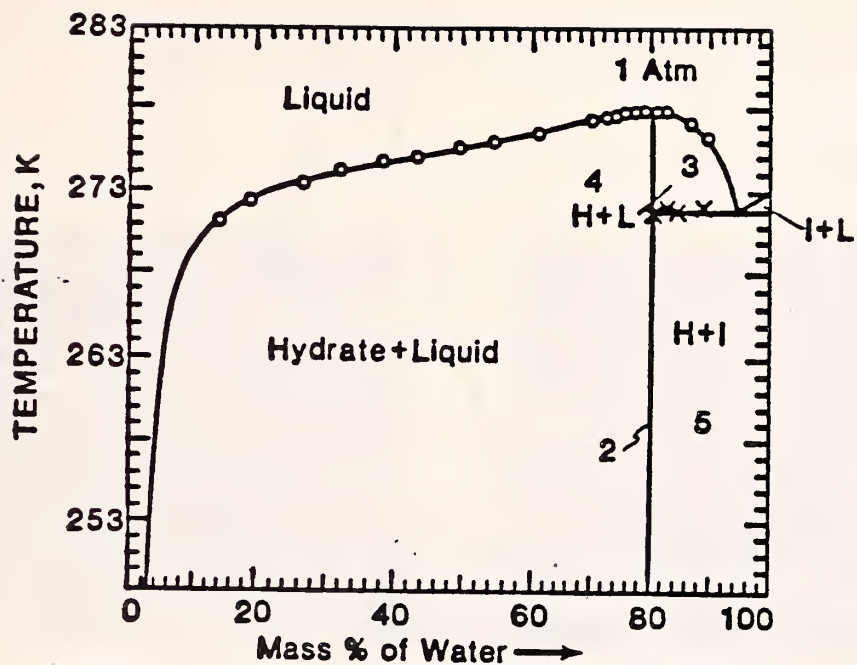


Figure 1. Phase diagram for tetrahydrofuran-water system at one atmosphere

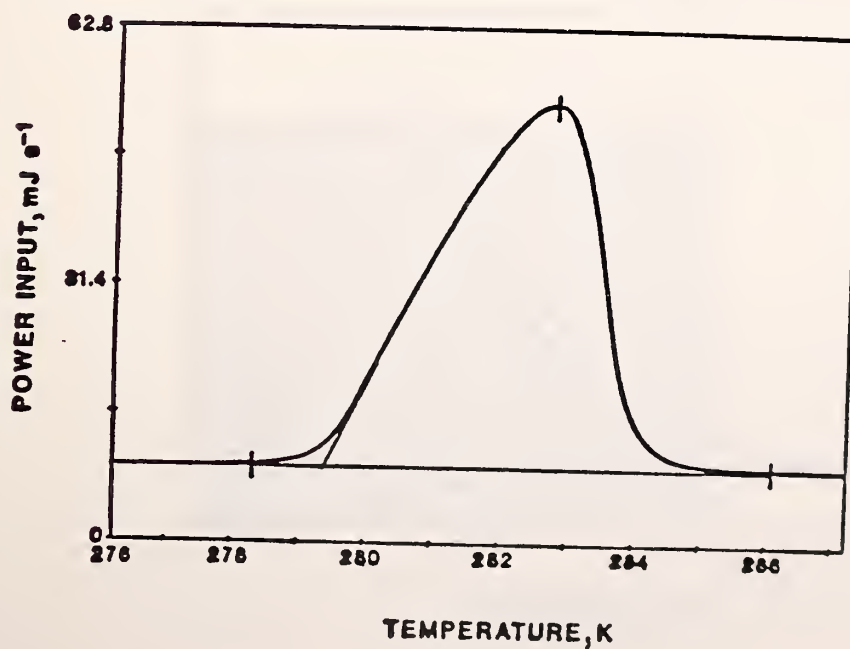


Figure 2. DSC scan typical of pure substance (hydrate only)

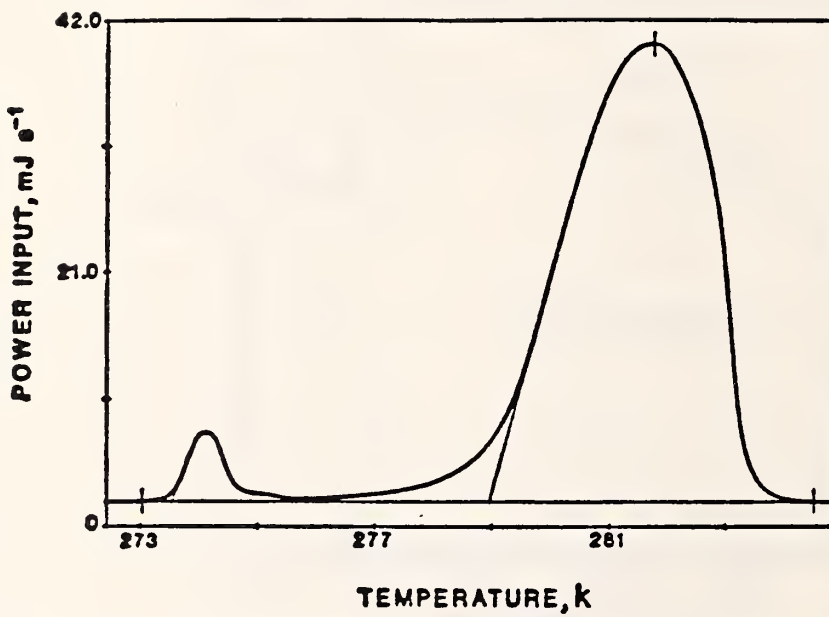


Figure 3. DSC scan of specimen from eutectic region

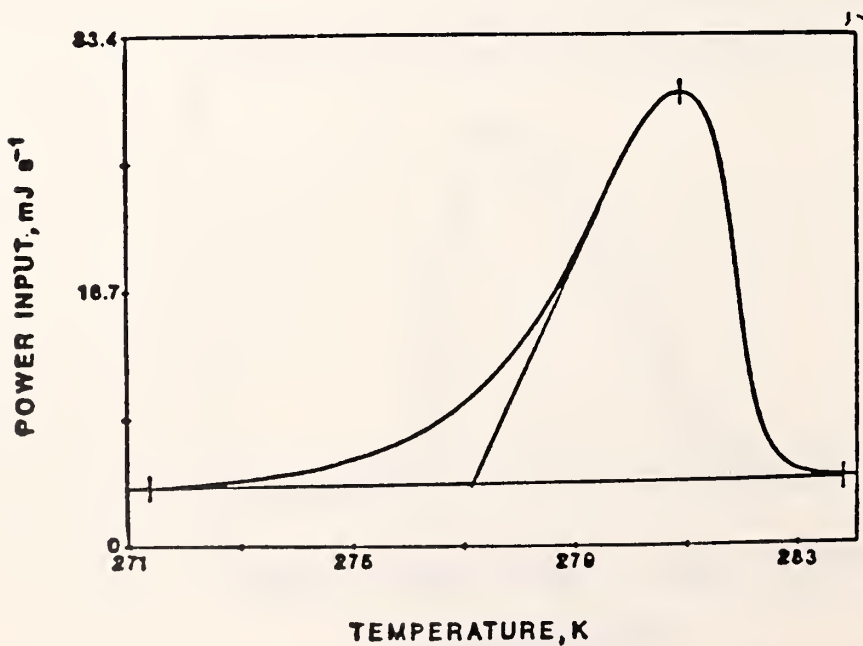
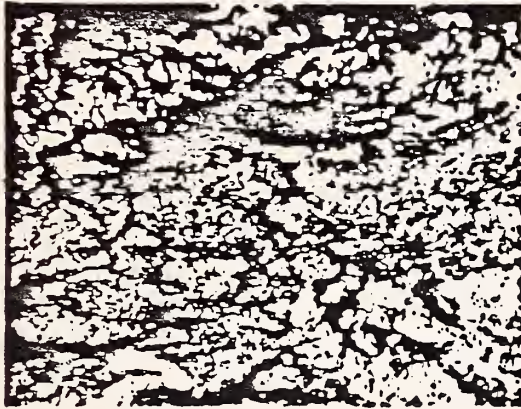
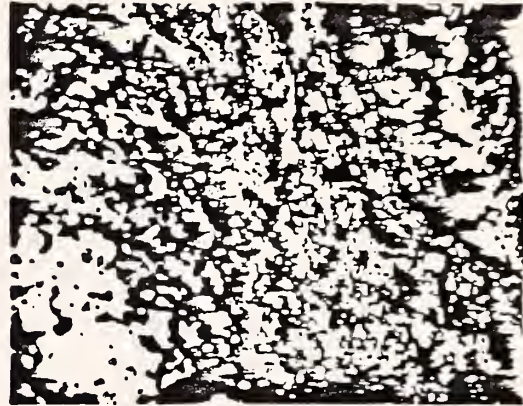


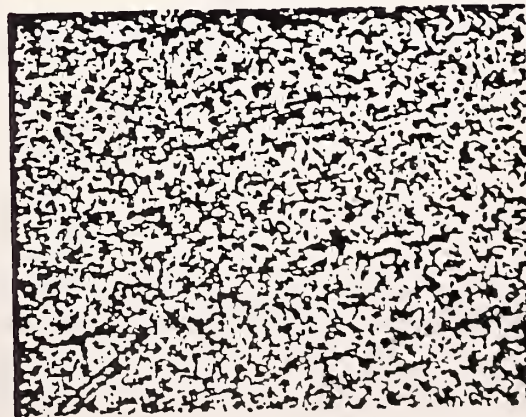
Figure 4. DSC scan of specimen showing premelting



Ethylene oxide



water



New pan

Figure 5. Photomicrographs of specimen pans illustrating deterioration (50X)

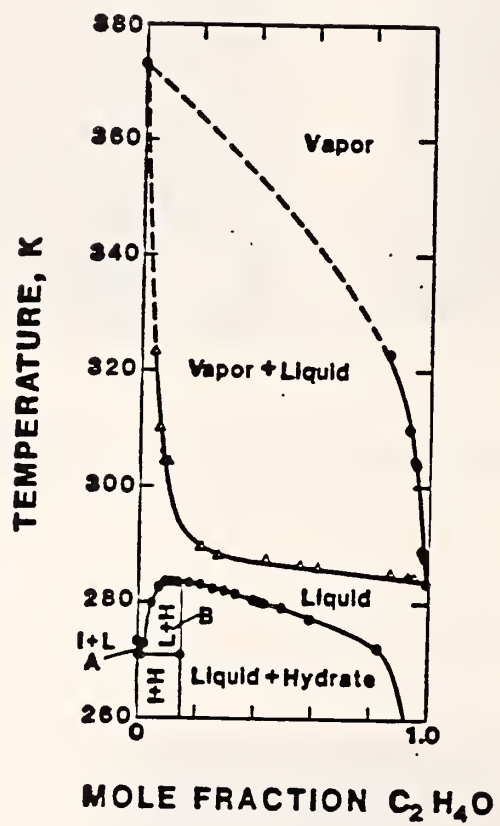


Figure 6. Phase diagram for ethylene oxide-water system (14, 15)

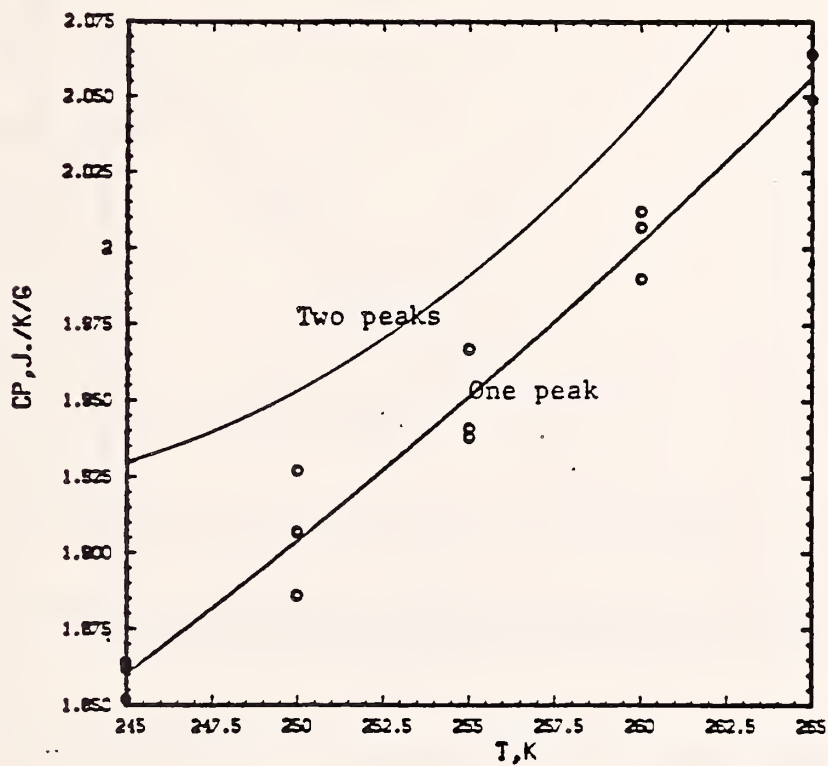


Figure 7. Heat capacity versus temperature-ethylene oxide hydrates

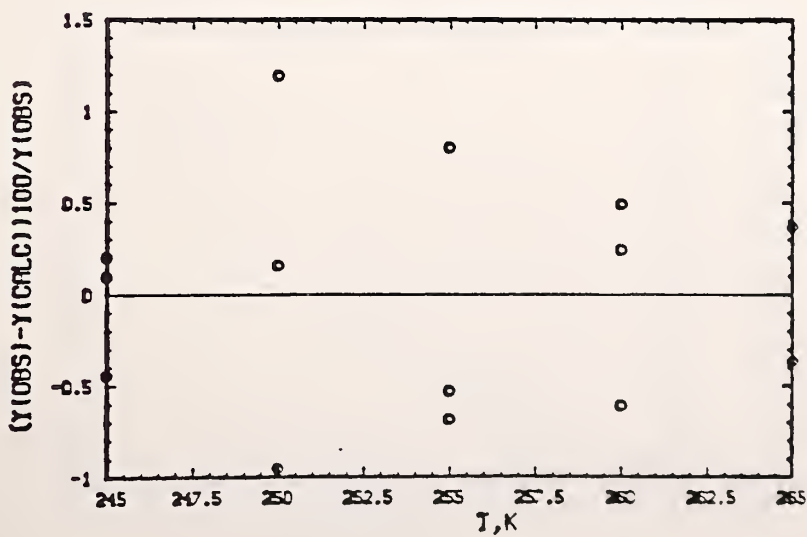


Figure 8. Deviation plot for ethylene oxide hydrates

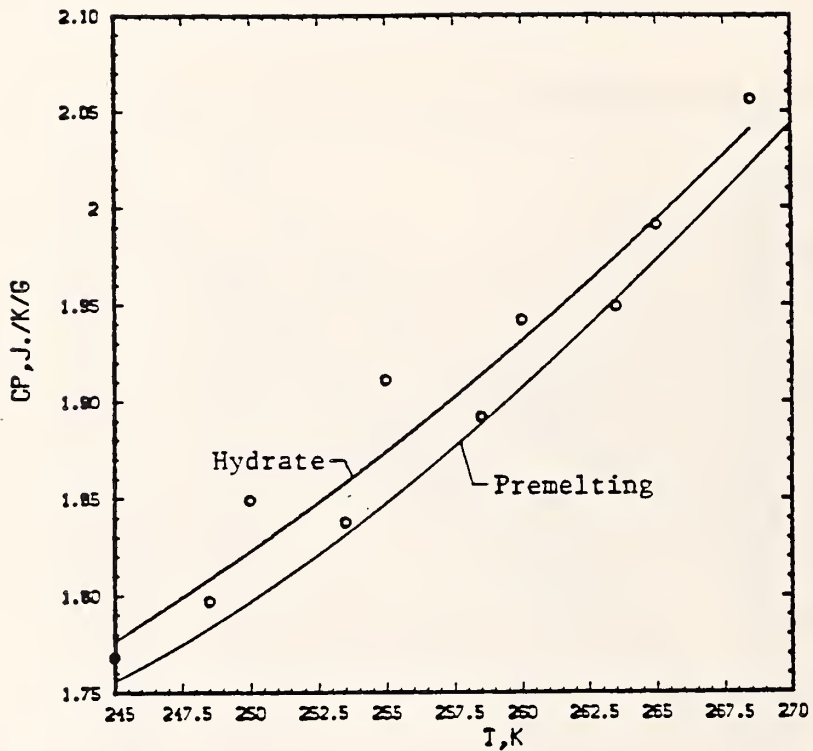


Figure 9. Heat capacity versus temperature - tetrahydrofuran hydrates

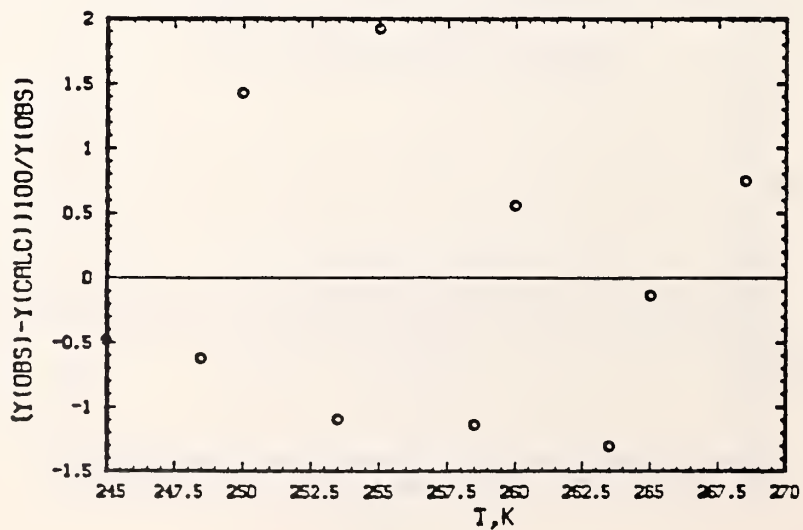


Figure 10. Deviation plot for tetrahydrofuran hydrates

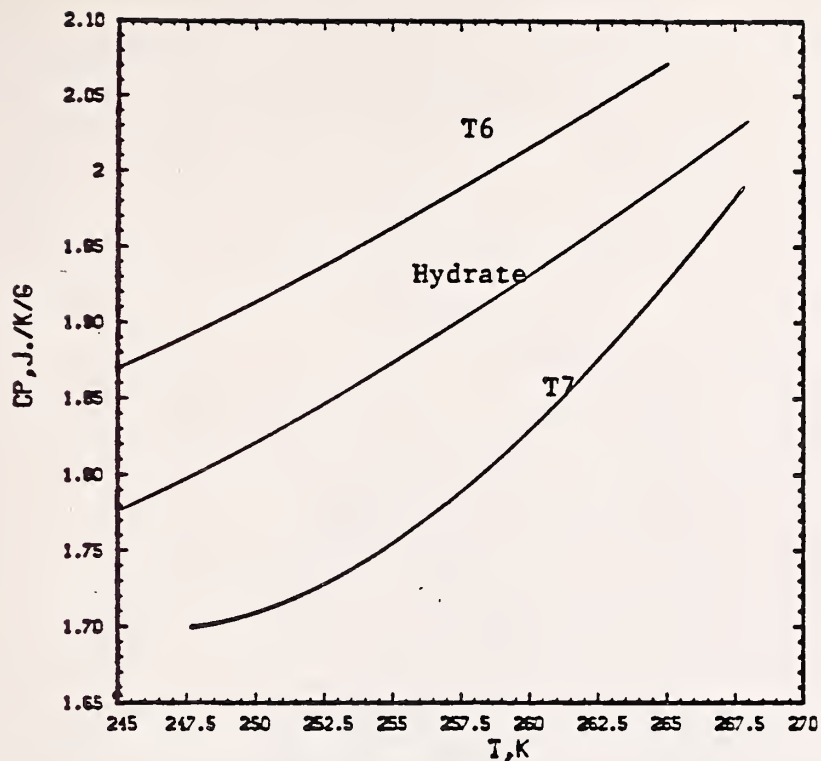


Figure 11. Heat capacity versus temperature-tetrahydrofuran eutectic mixtures

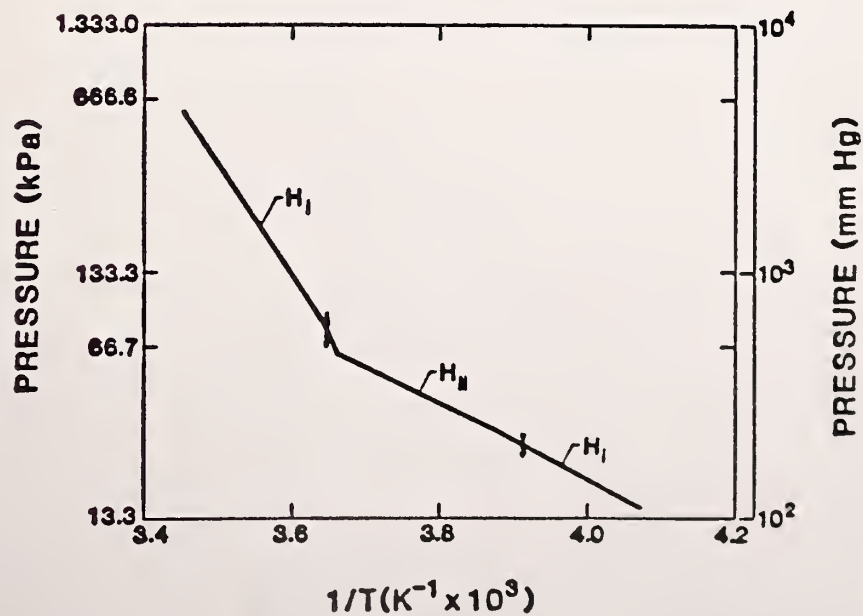
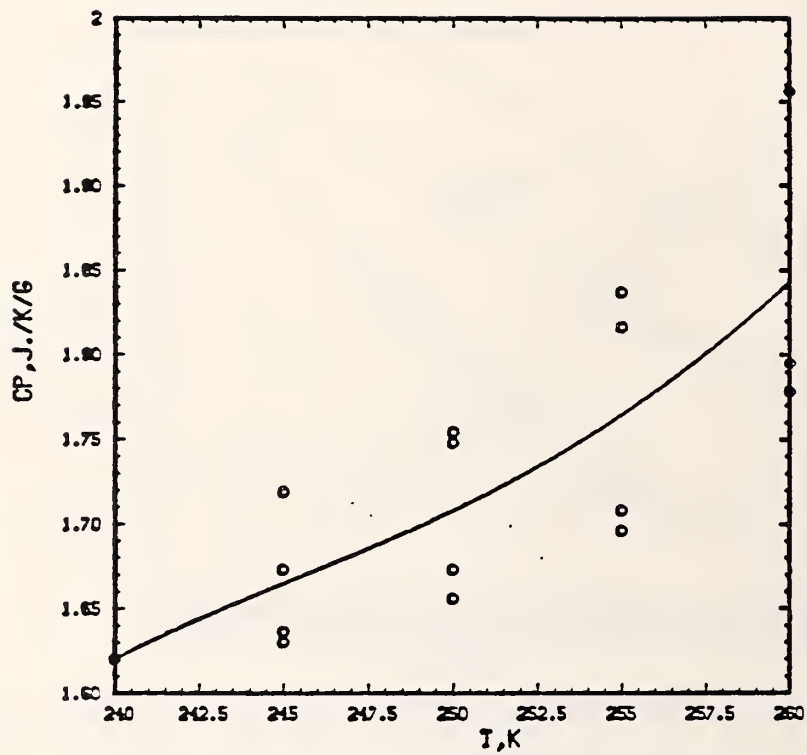
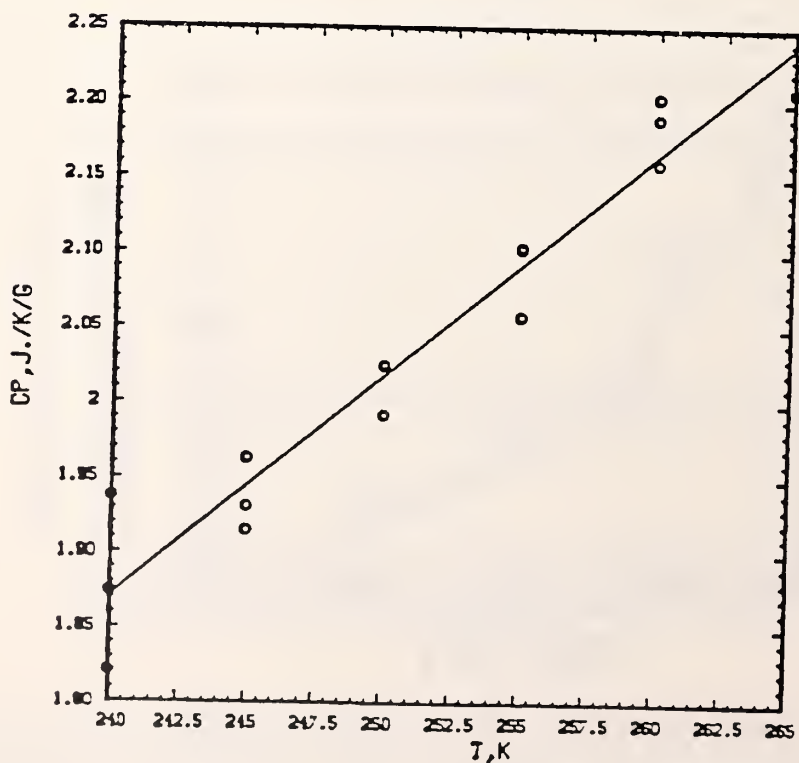


Figure 12. Dissociation pressure curve for cyclopropane hydrate



Cyclopropane hydrate I



Cyclopropane hydrate II

Figure 13. Heat capacity versus temperature-cyclopropane hydrates